

1-1-2014

# A Multi-Modal Continuous-Systems Model of a Novel High-Q Disk Resonator in a Viscous Liquid

Mohamad S. Sotoudegan  
mohamadsadegh.sotoudegan@marquette.edu

Stephen M. Heinrich  
*Marquette University*, stephen.heinrich@marquette.edu

Fabien Josse  
*Marquette University*, fabien.josse@marquette.edu

Isabelle Dufour  
*Université de Bordeaux*

Oliver Brand  
*Georgia Institute of Technology*

# A MULTI-MODAL CONTINUOUS-SYSTEMS MODEL OF A NOVEL HIGH-Q DISK RESONATOR IN A VISCOUS LIQUID

Mohamad S. Sotoudegan<sup>1</sup>, Stephen M. Heinrich<sup>1</sup>, F. Josse<sup>2</sup>, Isabelle Dufour<sup>3</sup>, Oliver Brand<sup>4</sup>

Depts. of<sup>1</sup>Civil, Construction and Environmental Engineering and <sup>2</sup>Electrical and Computer Engineering, Marquette University, Milwaukee, WI, USA; <sup>3</sup>Université de Bordeaux, Laboratoire IMS, UMR 5218, F-33400, Talence, France;

<sup>4</sup>School of Electrical and Computer Engineering, Georgia Institute of Technology, Atlanta, GA, USA

Presenter's e-mail address: [stephen.heinrich@marquette.edu](mailto:stephen.heinrich@marquette.edu)

## INTRODUCTION

To achieve higher quality factors ( $Q$ ) for liquid-phase sensing applications, several researchers have explored the use of in-plane modes in an effort to minimize coupling of the vibrating device with the surrounding liquid. Examples include axial and in-plane flexural modes of microcantilevers and, more recently, a novel disk-type device [1,2] actuated electrothermally via two tangentially oriented legs (Fig. 1a). In the latter device all surfaces of the resonator move primarily along a tangential direction, so that the interaction with the fluid is dominated by shear; as a result, unprecedented  $Q$  values near 300 in liquids were attained. The theory in those studies, however, was limited to finite element simulations. As a first step in understanding in more detail the underlying theory of this promising device, the present authors proposed a simple single-degree-of-freedom (SDOF) analytical model for free [3] and forced [4] vibrations and referred to such a device as an “all-shear interaction device,” or ASID. The SDOF model was based on the idealized system of Fig. 1b and the assumption that the legs behave as massless elastic

springs experiencing no fluid resistance. In the present paper we extend the earlier model by treating the legs as continuous axial members having distributed mass and stiffness and subjected to distributed resisting forces due to the surrounding fluid. As in the previous model, the disk is taken as rigid and subject to fluid resistance on all of its surfaces. Here we consider a harmonic “eigenstrain” in the legs due to electrothermal actuation which causes the disk rotation  $\theta$ , as was employed in the tests of [1,2] and in the SDOF model of [4]. The objectives of the present work are to expand our earlier model to include more realistic scenarios, to generate response functions that include multiple modes, and to examine the accuracy of the SDOF analytical results for the in-liquid resonant frequency and  $Q$  factor for mode 1. As will be seen, the simple SDOF results are in many cases in excellent agreement with those generated by the present model and reflect experimental trends over fairly wide ranges of system parameters; thus, they may be of use in understanding the behavior of ASID devices excited in their fundamental mode.

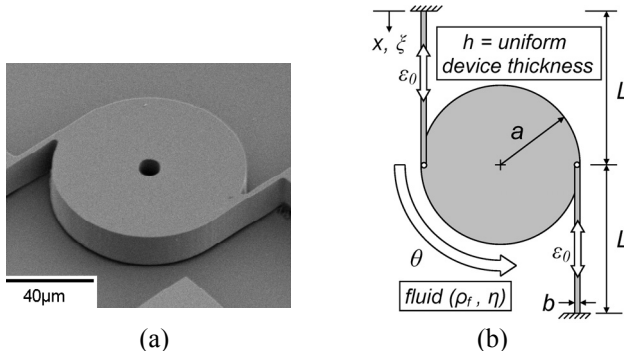


Fig. 1. (a) Silicon disk resonator with tangential support beams [1] (© 2010 IEEE); (b) Idealized system and notation.

## MATHEMATICAL FORMULATION & SOLUTION

In addition to the prior hypotheses, we assume that the local fluid resistance on any surface of the ASID is given by the solution of Stokes's second problem. This leads to the governing boundary value problem:

$$\begin{aligned} \bar{u}''(\xi, \tau) - \frac{\pi^{3/2}}{2} \sqrt{L_0 L} \left(1 + \frac{1}{b}\right) \bar{\omega}^{3/2} \dot{\bar{u}}(\xi, \tau) \\ - \frac{\pi^2}{4} \bar{\omega}^2 \left[1 + \frac{2}{\sqrt{\pi \bar{\omega}}} \sqrt{L_0 L} \left(1 + \frac{1}{b}\right)\right] \ddot{\bar{u}}(\xi, \tau) = 0, \end{aligned} \quad (1)$$

$$\bar{u}(0, \tau) = 0, \quad (2a)$$

$$\bar{u}'(1, \tau) + \frac{\pi^3}{16} \frac{\bar{a}^2}{\bar{b} \bar{L}} \left\{ \bar{\omega}^2 \left[ 1 + \frac{2}{\sqrt{\pi \bar{\omega}}} \sqrt{\bar{L}_0 \bar{L}} \left( 1 + \frac{2}{\bar{a}} \right) \right] \ddot{\bar{u}}(1, \tau) + \frac{2}{\sqrt{\pi}} \sqrt{\bar{L}_0 \bar{L}} \left( 1 + \frac{2}{\bar{a}} \right) \bar{\omega}^{3/2} \dot{\bar{u}}(1, \tau) \right\} = \varepsilon_0 e^{i\tau}, \quad (2b)$$

$$\begin{aligned} \bar{u} &\equiv u/L, \quad \xi \equiv x/L, \quad \tau \equiv \omega t, \quad \bar{\omega} \equiv \omega/\omega_0, \\ \omega_0 &\equiv \pi \sqrt{E/\rho}/2L, \quad \bar{a} \equiv a/h, \quad \bar{b} \equiv b/h, \quad (3a-i) \\ \bar{L} &\equiv L/h, \quad \bar{L}_0 \equiv L_0/h \equiv \sqrt{\rho_f^2 \eta^2 / E \rho^3 / h}. \end{aligned}$$

The system parameters are  $h$ =device thickness,  $(b, L)$  =leg width and length,  $a$ =disk radius,  $(E, \rho)$ =Young's modulus of legs and density of device,  $(\eta, \rho_f)$ =viscosity and density of liquid. Actuation parameters are  $(\varepsilon_0, \omega)$ =electrothermal eigenstrain amplitude and frequency, while the response quantity is the axial displacement,  $u(\xi, \tau)$ , in each leg,  $\xi$  and  $\tau$  being dimensionless axial and time coordinates. Primes and dots denote differentiation w.r.t.  $\xi$  and  $\tau$ . The solution due to the eigenstrain,  $\varepsilon_0 e^{i\tau}$ , is  $\bar{u}(\xi, \tau) = \varepsilon_0 \bar{U}(\xi) e^{i\tau}$ , where

$$\begin{aligned} \bar{U}(\xi) &= \frac{\sin \lambda \xi}{\lambda \cos \lambda - \frac{\pi^3 \bar{a}^2 \bar{\omega}^2 \sin \lambda}{16 \bar{b} \bar{L}} \left[ 1 + 2(1-i) \left( 1 + \frac{2}{\bar{a}} \right) \sqrt{\frac{\bar{L}_0 \bar{L}}{\pi \bar{\omega}}} \right]}, \\ \lambda &= \frac{\pi \bar{\omega}}{2} \left[ 1 + 2(1-i) \left( 1 + \frac{1}{\bar{b}} \right) \sqrt{\frac{\bar{L}_0 \bar{L}}{\pi \bar{\omega}}} \right]^{1/2}. \end{aligned} \quad (4a, b)$$

The disk rotation and axial leg strain at the support, two output signals of interest, are

$$\theta(\tau) = \frac{\varepsilon_0 L}{a} \bar{U}(1) e^{i\tau}, \quad \varepsilon_x^{(\text{supp.})}(\tau) = \varepsilon_0 \bar{U}'(0) e^{i\tau}. \quad (5a, b)$$

### NUMERICAL RESULTS

Results of the model are shown in Figs. 2-4. For the cases shown, the two output signals give identical mode-1 responses but differ significantly for higher modes, the strain signal being stronger (Fig. 2); the accuracy of the SDOF formula for mode-1 resonant frequency [3,4] is excellent for  $a/h \geq 0.5$  (Fig. 3);  $Q$  results based on the SDOF formula [3,4] are in very good agreement with the present model, with both models capturing the experimental trends of [2] w.r.t.  $a/h$  and  $b/L$  (Fig. 4). Additional results and discussion will be provided during the presentation.

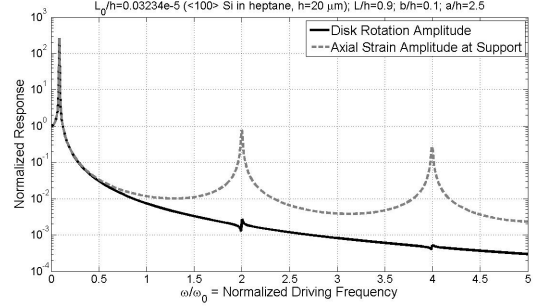


Fig. 2. Multi-modal response based on two output signals: disk rotation (solid) and axial strain at support (dashed).

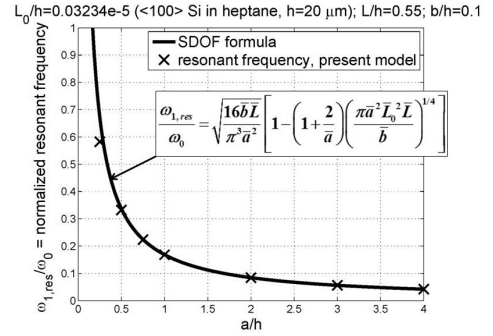


Fig. 3. Normalized mode-1 resonant frequency: present model (markers) and SDOF analytical formula [4].

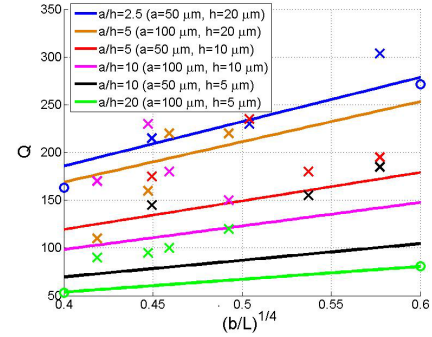


Fig. 4.  $Q$  results: data (X) for heptane [2], SDOF formula (lines) [4], present model by bandwidth method (O).

### REFERENCES

- [1] A. Rahafrooz and S. Pourkamali, "Rotational mode disk resonators for high-Q operation in liquid," *IEEE Sens. Conf.*, 1071-1074, 2010.
- [2] A. Rahafrooz and S. Pourkamali, "Characterization of rotational mode disk resonator quality factors in liquid," *IEEE IFCS*, 5 pp., 2011.
- [3] M. Sotoudegan, S.M. Heinrich, F. Josse, N.J. Nigro, I. Dufour, and O. Brand, "A simple model for the in-plane rotational response of a disk resonator in liquid: resonant frequency, quality factor, and optimal geometry," *NMC 2013*, Stanford, CA, 107-108, 2013.
- [4] M. Sotoudegan, S. Heinrich, F. Josse, N. Nigro, I. Dufour, and O. Brand, "Effect of design parameters on the rotational response of a novel disk resonator for liquid-phase sensing: analytical results," *IEEE Sens. Conf.*, 1164-1167, 2013.